Eur. Phys. J. D **45**, 507–514 (2007)
DOI: 10.1140/epjd/e2007-00200-0

THE EUROPEAN PHYSICAL JOURNAL D

Structure and optical properties of Na clusters deposited on MgO(001)

M. Bär[1], L.V. Moskaleva[2], M. Winkler[2], P.-G. Reinhard[1,3,a], N. Rösch[2], and E. Suraud[3]

[1] Institut für Theoretische Physik, Universität Erlangen, Staudtstrasse 7, 91058 Erlangen, Germany
[2] Department Chemie, Theoretische Chemie, Technische Universität München, 85748 Garching, Germany
[3] Laboratoire de Physique Théorique, Université P. Sabatier, 118 route de Narbonne, 31062 Toulouse Cedex, France

Received 1st February 2007 / Received in final form 24 May 2007
Published online 20 June 2007 –

Abstract. We present a hierarchical model for describing Na clusters which interact with a MgO(001) surface. The clusters are treated by time-dependent density-functional theory in full detail and the substrate by classical dynamics of Mg and O ions including dynamical polarizability. The model is calibrated to accurate all-electron density-functional model calculations of a Na adsorbate on an extended model of the MgO(001) surface. We show first applications to structure and optical response of $Na_N MgO$ adsorption complexes for $N = 3 \ldots 8$. The overall shape of the metal clusters is hardly changed by the interaction of the cluster with the surface while the detailed structure is slightly distorted to accommodate surface corrugation. The peak positions of the Mie plasmon resonances are not shifted, but the spectral fragmentation is strongly influenced by the surface.

PACS. 36.40.Gk Plasma and collective effects in clusters – 36.40.Mr Spectroscopy and geometrical structure of clusters – 36.40.Sx Diffusion and dynamics of clusters – 36.40.Vz Optical properties of clusters

1 Introduction

Clusters at surfaces represent a promising and rich field of research. Surfaces constitute a useful laboratory for all sorts of chemical reactions [1–5]. Clusters as finite pieces of rather homogeneous material are interesting objects for fundamental studies and for applications in nano-science, see e.g. [6,7]. The combination of both creates a world of new possibilities. In this paper, we concentrate on the interaction of a metal cluster with an insulating surface of a fairly rigid material. Metal clusters are prototypes of finite Fermion systems, distinguished by their shared valence electron cloud which leads to pronounced quantum effects and collective resonances (Mie plasmon) [8]. They have also practical appeal, e.g. in catalysis [1,4,9]. The attachment to insulators leaves the electronic structure of a cluster basically intact, but may polarize the electronic charge distribution depending on the interface interaction. Soft interfaces, as provided by rare-gases, exert only small perturbations and are often used for handling and storage of clusters in nearly free state. Strong interactions with an interface induce larger rearrangements thus producing new effects, as e.g. second-harmonic generation [10] or planarization of clusters [11,12]. These strong interactions are usually related to robust materials more suited for practical applications. Previously, we extensively studied soft substrates (see e.g. [13,14]). Now, we are extending our computational explorations to solid interfaces and take MgO(001) as a first test case in that regime. We will investigate the structure and the optical response of small Na clusters interacting with the surface MgO(001).

A rigorous quantum mechanical description of an adsorption system with at least two components of quite different physical and chemical nature, e.g. a metal particle and an oxide surface of (formally) infinite dimensions, presents a challenge for theory. As in other large-scale problems, one has to resort to hierarchical modeling where only a small, and most active, part of the system is described in full quantum-mechanical detail while more distant and/or more inert parts are handled at a more approximate level with less expensive methods, often with a classical description based on an atomistic model of the interactions, i.e. molecular mechanics or molecular dynamics (MD). Examples are the quantum-mechanical plus molecular-mechanical approach often used in bio-molecules, see e.g. [15], or in surface science where the active site of a chemical reaction (i.e. adsorbed atoms or molecules together with the adsorption site) is embedded in an environment which is described by classical mechanics, e.g. with a "shell model" [16,17].

[a] e-mail: reinhard@theorie2.physik.uni-erlangen.de

Table 1. The degrees of freedom of the model. Upper block: Na cluster. Lower block: active cell of the MgO substrate.

$\varphi_n(\boldsymbol{r})$, $n = 1, ...N_{\rm el}$	valence electrons of the Na cluster
$\boldsymbol{R}_{i^{(\rm Na)}}$, $i^{(\rm Na)} = 1...N_{\rm i}$	positions of the Na^+ ions
$\boldsymbol{R}_{i^{(c)}}$, $i^{(c)} = 1...M$	positions of the O cores
$\boldsymbol{R}_{i^{(v)}}$, $i^{(v)} = 1...M$	center of the O valence cloud
$\boldsymbol{R}_{i^{(k)}}$, $i^{(k)} = 1...M$	positions of the Mg^{2+} cations

Recently, we successfully applied such a hierarchical model to Na clusters in/on a rare-gas substrate [13,14,18]. We are now going to extend that approach to a MgO substrate which is insulating and fairly rigid and interacts more strongly with an adsorbate. The Na cluster as the most reactive part is treated by quantum mechanics using the time-dependent local-density approximation (TDLDA) for the valence electrons and MD for the ions, for details see [19,20]. The electronically inert substrate is described classically taking its dynamical polarizability into account. The coupling is achieved by polarization potentials and local pseudo-potentials. These are calibrated by comparison with accurate quantum chemical calculations along the lines of [17]. The very efficient modeling presented in the following will allow large-scale surveys. We start here with studying structure and linear response of small Na_N clusters for $N = 3...8$. The key interest lies in the degree of perturbation induced by the MgO(001) surface.

2 The hierarchical cluster-surface model

2.1 Constituents

The hierarchical modeling for Na clusters interacting with the surface MgO(001) is developed in analogy to earlier studies of Na clusters interacting with an Ar substrate, for a detailed protocol see [21]. The Na cluster is treated in standard fashion [19,20]. Valence electrons are described as single-particle wavefunctions $\varphi_n(\boldsymbol{r})$ and the complementing Na^+ ions are handled as charged classical point particles characterized by their positions $\mathbf{R}_{i^{(\rm Na)}}$, see upper block of Table 1. The substrate is composed of two types of species whose properties are formed in the context of bulk structure: Mg^{2+} cations and O^{2-} anions. The cations are electrically inert and can be treated as charged point particles; they are labeled by $i^{(k)}$. The anions are easily polarizable and are handled in terms of two constituents: a valence electron distribution (labeled by $i^{(v)}$) and the complementing core (labeled by $i^{(c)}$). Each of these three types of constituents is described in terms of positions $\boldsymbol{R}_{i^{(\rm type)}}$. The difference $\mathbf{R}^{(c)} - \mathbf{R}^{(v)}$ describes the electrical dipole moment of the O^{2-} anion. These (classical) degrees of freedom are summarized in the lower block of Table 1. The Mg and O ions reside in an active cell of the MgO(001) surface region underneath the Na cluster. The cell consists of three layers, each containing square arrangements of $Mg_{242}O_{242}$. To avoid the Coulomb singularity and to simulate the finite extension of these constituents, we associate a smooth charge distribution $\rho(\boldsymbol{r}) \propto \exp(-\boldsymbol{r}^2/\sigma^2)$ with each of these ionic centers. This yields a soft Coulomb potential (3c) to be used for all active particles. The width parameters σ_c, σ_v, and σ_k are adjusted to the response properties of the MgO(001) substrate. The active cell is surrounded by an infinitely extended outer region of spectators, whose effect on the active part is given by a time-independent shell-model potential, see below.

2.2 Energy

Starting point is the total energy

$$E = E_{\rm Na} + E_{\rm MgO} + E_{\rm coupl} \tag{1}$$

where $E_{\rm Na}$ describes an isolated Na cluster, $E_{\rm MgO}$ the MgO(001) substrate, and $E_{\rm coupl}$ the coupling between the two subsystems. For $E_{\rm Na}$, we take the standard TDLDA-MD functional as in previous studies of free clusters [19,20]. It is composed of an LDA functional for the electrons, including an average self-interaction correction [22], the point-charge Coulomb energy of the Na^+ ions, and an electron-ion coupling in the form of soft local pseudo-potentials [23].

The energy of the MgO(001) surface is modeled by a three-layer slab in close analogy to [17]. The surface has translational symmetry in directions parallel to surface. The long-range Coulomb interaction requires inclusion of remote sites. To this end, we distinguish between an active cell close to the deposited cluster and an outer region of "spectators". Just as the active cell, the outer region comprises O cores and O valence clouds as well as Mg^{2+} cations. However, they are kept "frozen" at the positions of the free MgO surface. We assign the labels $i^{(C)}$, $i^{(V)}$, and $i^{(K)}$ to them running, in principle, over an infinite manifold of periodic copies in the two horizontal directions and the vertical layers below the surface. The constituents of the active cell are explicitly excluded from this set. The various charges in this outer region produce a Coulomb field

$$\Phi'_{\rm out}(\boldsymbol{r}) = \sum_{i^{(A)} \in \{C,V,K\}} \frac{q_A e^2}{|\boldsymbol{r} - \boldsymbol{R}_{i^{(A)}}|} \tag{2}$$

which also influences the cluster and the centers inside the active cell. One can model centers in surrounding cells as point charges because the effect of local smoothing is of very short range. This, in turn, allows one to use analytical techniques similar to Ewald summation [24,25]. The shell potential $\Phi'_{\rm out}$, being time-independent, is computed in great detail at the start of the calculations and tabulated for continued use. The boundary region of the active cell will also feel some effect of the short-range core repulsion (3d) of neighboring atoms in the outer region [17]. We take that into account by freezing the ionic positions at the boundary.

The energy of the MgO subsystem is then

$$E_{\mathrm{MgO}} = \sum_{i^{(\alpha)}\in\{c,v,k\}} q_\alpha \Phi'_{\mathrm{out}}(\boldsymbol{R}_{i^{(\alpha)}}) + \frac{1}{2}\sum_{i^{(\alpha)}j^{(\beta)}\in\{c,v,k\}} V_{\alpha\beta}(r_{i^{(\alpha)}j^{(\beta)}}) + \sum_{i^{(c)}}\left[\frac{\kappa}{2} r^2_{i^{(c)}i^{(v)}} - V_{\alpha\beta}(r_{i^{(c)}i^{(v)}})\right] \quad (3a)$$

$$V_{\alpha\beta}(r) = q_\alpha q_\beta V_{\mathrm{soft}}(r,\sigma_{\alpha\beta}) + f_{\alpha\beta}(r) \quad (3b)$$

$$V_{\mathrm{soft}}(r,\sigma) = e^2\frac{\mathrm{erf}(r/\sigma)}{r} \quad (3c)$$

$$f_{\alpha\beta}(r) = a_{\alpha\beta}\exp\left(-\frac{r}{\lambda_{\alpha\beta}}\right) - \frac{b_{\alpha\beta}}{r^6} \quad (3d)$$

$$r_{IJ} = |\boldsymbol{R}_J - \boldsymbol{R}_I| \quad (3e)$$

$$\sigma_{\alpha\beta} = \sqrt{\sigma_\alpha^2 + \sigma_\beta^2}. \quad (3f)$$

In line 3 of equation (3a), the Coulomb potential between core- and valence charges at the same site is replaced by a harmonic oscillator potential which correctly reproduces the dielectric response. Label $i^{(v)}$ identifies the O^{2-} valence electron distribution at the site of the core $i^{(c)}$. The potential V_{soft} comprises Coulomb interactions while $f_{\alpha\beta}$ accounts for short-range repulsion and Van-der-Waals attraction.

The coupling to the cluster is predominantly established by the Coulomb field of the substrate (active cell as well as outer region). At short distances, the core repulsion has to be added in the form of appropriate short-range potentials. The coupling energy becomes

$$E_{\mathrm{coupl}} = E_{\mathrm{MgONa^+}} + \int d^3r n_{\mathrm{el}}\left[\Phi'_{\mathrm{out}} + V_{\mathrm{MgOel}}\right] \quad (4a)$$

$$E_{\mathrm{MgONa^+}} = \sum_{j^{(\mathrm{Na})}}\left[\Phi'_{\mathrm{out}}(r_{j^{(\mathrm{Na})}}) + \sum_{i^{(\alpha)}=\{c,v,k\}} V_{\mathrm{act},\alpha}(r_{i^{(\alpha)}j^{(\mathrm{Na})}})\right] \quad (4b)$$

$$V_{\mathrm{act},\alpha}(r) = q_\alpha V_{\mathrm{soft}}(r,\sigma_{\alpha\mathrm{Na}}) + \frac{A'_\alpha}{1+e^{(r-w_\alpha)/C'_\alpha}} - D'_\alpha\left(\frac{\mathrm{erf}(\frac{r}{\Lambda'_\alpha})}{r}\right)^8 \quad (4c)$$

$$V_{\mathrm{MgOel}}(\boldsymbol{r}) = \sum_{i^{(\alpha)}=\{c,v,k\}}\left[q_\alpha V_{\mathrm{soft}}(r,\sigma_\alpha) + \frac{A_\alpha}{1+\exp[(|\boldsymbol{r}-\boldsymbol{R}_{i^{(\alpha)}}|-B_\alpha)/C_\alpha]}\right]. \quad (4d)$$

2.3 Calibration

The energy-functional E_{Na} of the Na cluster is the same as used in previous studies on free clusters [19,20]. The model E_{MgO} of the substrate is adapted from the well established shell-model description [17]. The as yet open model parameters A_α, B_α, C_α, A'_α, C'_α, D'_α, w_α and Λ'_α of the coupling energy E_{coupl} are adjusted for the case of a single Na atom and Na^+ ion interacting with MgO(001). To that end, we computed the Born-Oppenheimer (BO) energy as function of the distance of a sodium atom or ion to the MgO(001) surface [26] using an all-electron local density description of a model "cluster" embedded in an elastic polarizable environment (EPE) [17]. The substrate is partitioned into a relatively small subsystem near the adsorbate which is treated with an all-electron quantum mechanical method and the remaining part which is handled in the classical polarizable model. The small part is called "QM cluster" in the original literature. We use here the notion QM subsystem to avoid confusion with the real cluster (=nano-particle) which we treat later on. The entire substrate model was chosen to comprise a total of 280 ions (QM subsystem + environment) and a surface charge density which represented the electrostatic field of the infinite crystal. The QM subsystem contained 12 O and 12 Mg centers, terminated by 12 additional Mg pseudo-potentials at the subsystem boundaries. The near environment of the EPE model was represented by a finite part of a two-layer slab with 244 ions, excluding the inner QM subsystem of 36 ions. The electrostatic field of the remaining (infinite) region was represented by a surface charge distribution on a sphere of radius 11 a.u., represented by a set of 128 point charges. The calculations were carried out with the linear combination of Gaussian-type orbitals fitting-functions density functional method [27] as implemented in the computer code ParaGauss [28,29]. The Kohn-Sham wave functions were represented as linear combinations of Gaussian-type functions. For the MgO substrate, the set of Gaussian basis sets were chosen as in previous studies [17]. The basis set of Na was adapted from [30]; see also [26]. For further computational details, in particular on the EPE embedding scheme, see [17].

We considered four straight BO paths in (001) direction: one towards a Mg site, one towards an O site, one at a bridge site between Mg and O, and a last one at a hollow site. Along these four paths, we compared the ab-initio results for total energy and for the single-electron energy of the occupied valence electron state in the Na atom with the results of the present simplified model and the parameters were tuned to yield best agreement. Note that the repulsive part of the BO energies at close distances does not go very far yet. We are encountering here a weakness of the ab-initio calculation which employs a gradient-corrected exchange-correlations functional [31, 32]. Similar to LDA, gradient-corrected functionals are known to underestimate band gaps and thus would underestimate the repulsion in the deep contact regime. We stay on the safe side and parameterize the reliable part of the ab-initio results. As a counter-check, we have have computed the electron transmission barrier (7.0 eV), into the MgO substrate and compared it with the empirically determined value (6.9 eV) [33]. Apparently, that value is well reproduced.

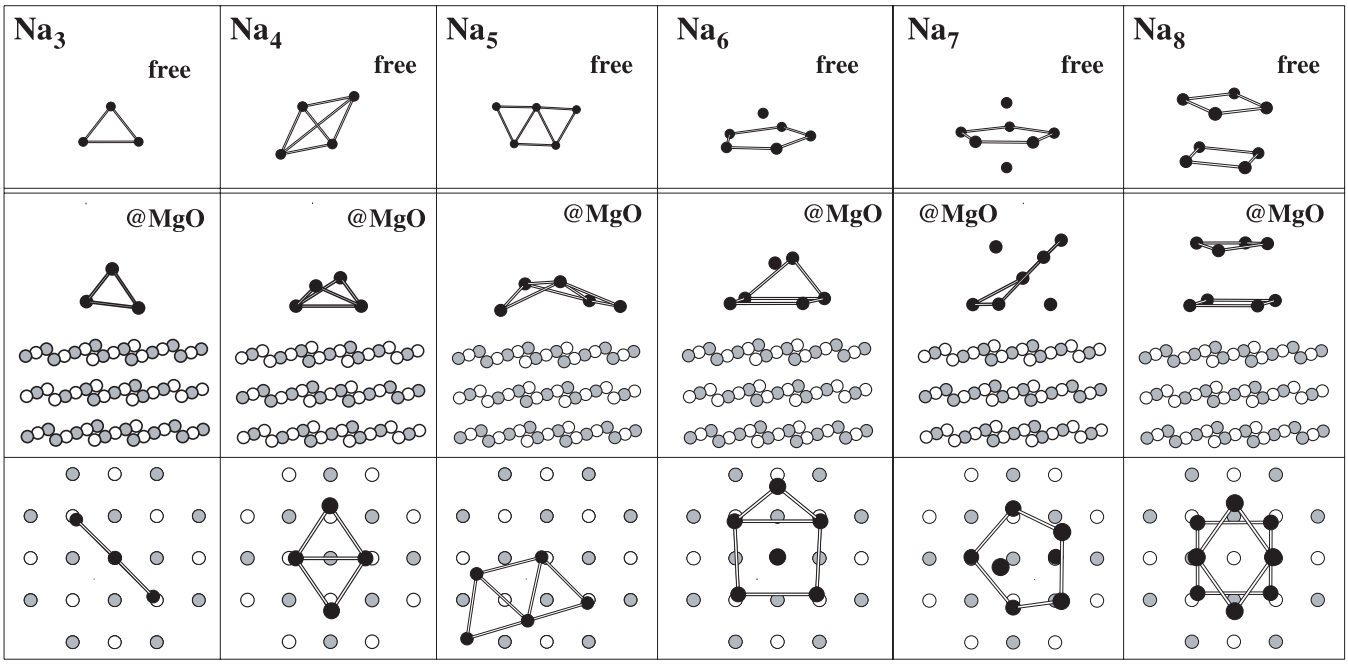

Fig. 1. Configurations of free (upper panel) and deposited (lower two panels) Na_N clusters. The lowest panels view the combined system from the top. The panels in the middle row show a slightly rotated side view. Na^+ centers are indicated by black circles, O^{2-} by open circles, and Mg^{2+} by grey circles. Bonds within the Na_N clusters are drawn to indicate connected sub-units.

2.4 Practical procedure

The numerical solution of the coupled quantum-classical system proceeds similar to [13,14]. The electron wavefunctions and spatial fields are represented on a Cartesian grid in three-dimensional coordinate space. The spatial derivatives are evaluated via fast Fourier transformation. The ground state configurations were found by accelerated gradient iteration for the electronic wavefunctions [34] and simulated annealing for the ions in the cluster and the substrate. The determination of ground state configurations required patience. We repeated the procedure several times for different initial conditions (deposition site, orientation, cluster shape) to explore the landscape of isomers and to pick the lowest isomer. Propagation is done by the time-splitting method for the electronic wavefunctions [35] and by the velocity Verlet algorithm for the classical coordinates of Na^+ ions and MgO constituents. The optical absorption spectra were computed by starting from the stationary ground state, initializing dynamics by an instantaneous dipole boost, recording the emerging time-evolution of the dipole moment $D(t)$, and finally Fourier transforming $D(t)$ to the frequency domain [20,36]. This efficient modeling yields a dramatic reduction of computational expense. All following results had been computed on simple workstations with Pentium IV 3 GHz processors.

3 Results

3.1 Structure

Figure 1 summarizes the structures determined for deposited neutral clusters up to nuclearity $N = 8$. The structures of the analogous free clusters are shown for comparison. The geometry of small free Na clusters is dictated by electronic shell effects [19]. Na_8 with a closed shell of $N_{el} = 8$ electrons is almost spherical. Lowering N_{el} drives structures to oblate shapes and for even lower N_{el} to triaxiality which means here fully planar Na_5 and Na_4. Na_3 is, of course, trivially planar. Most deposited clusters are distorted as we can see from the middle panels of Figure 1. The originally planar clusters Na_4 and Na_5 are placed parallel to the surface, but surface corrugation slightly destroys planar symmetry. Similarly, the bottom ring of Na_6 is stretched; its then remote edge is lifted up, almost to the height of the former top ion. Na_8, however, practically maintains its shape due to its magic electron shell and due to a fortuitous geometric matching with attractive sites on the surface. There is, of course, not much variation of shape for the triangle Na_3. It is noteworthy, however, that this system prefers a vertical orientation rather than a purely horizontal alignment. The reason becomes clear when looking at the top views in the bottom left panel. The O^{2-} sites (open circles) attract the Na^+ ions while the Mg^{2+} ions repel them. Two of the Na^+ ions fit attractive places. The next O^{2-} would be too far for the third ion. Thus it is advantageous to place that one out of the way in vertical direction. This vertical orientation of the adsorption complex is reminiscent of the structures determined for coinage metal dimers and trimers (M = Cu, Ag, Au) [37].

The same balance explains the crumpling for the larger clusters. Na_4 is close to matching four attractive sites, but the slight mismatch lets the ions feel the corrugation. The curious geometry of Na_5 is surprisingly well conserved in the top view, of course, again with some corrugation.

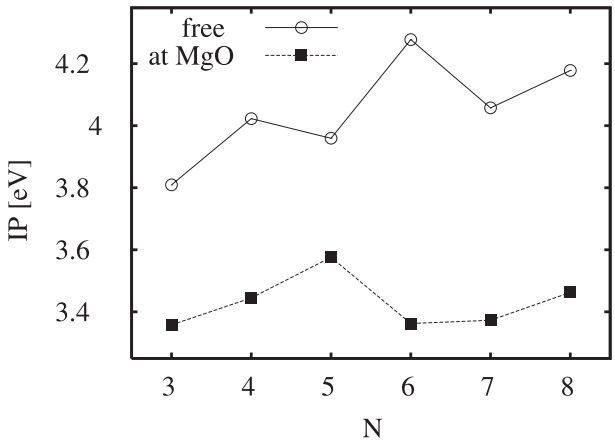

Fig. 2. Ionization potentials (IP) of free (open boxes) and deposited (filled boxes) Na_N clusters.

The angles of the fivefold ring of Na_6 and Na_5 represent rather soft modes and hence adapt easily to find a compromise between surface attraction and repulsion. For Na_8 we see a nice matching. The fourfold geometry is conserved upon adsorption because it is also present in the surface MgO(001). The orientation maximizes contacts with attractive sites, but they are not exactly matched which demonstrates the interplay between Na-Na distances and MgO geometry. The Na binding obviously overrules the interface interaction. This finding is also known for transition metal clusters adsorbed at MgO [5,38,39].

Truly weakly interacting surfaces as those of condensed rare gases just tie a cluster to the surface while leaving its structure essentially unperturbed. The MgO interface exhibits a stronger interaction. It can overrule weak features of the deposited clusters (e.g. bond angles), but stays still below the strength of metal-metal bonding within the cluster. Former studies have shown that NaCl surfaces yield stronger interface effects. They are able to overrule cluster binding such that planar clusters become always the ground state configuration even for the magic Na_8 [12]. A more detailed comparison with NaCl is beyond the scope of this paper and will be postponed to a subsequent publication.

Most of the spatial configurations of cluster ground states in Figure 1 keep approximately their symmetry. One obtains easily isomers by applying symmetry operations as, e.g., horizontal rotation by 90°. It so becomes obvious that there are usually many, energetically very close lying isomers (in the range of room temperature). Most of these symmetry-generated isomers are very similar in structure such that the above discussion is sufficiently general. There are other isomers with more different geometries. A systematic study of these will follow in subsequent publications.

The ionization potentials (IP) are an indicator for the binding of the valence electrons in the cluster (Fig. 2). IPs of deposited clusters are about 15% smaller than the corresponding results for clusters in the gas phase. That effect and order is similar to what we found at rare gas

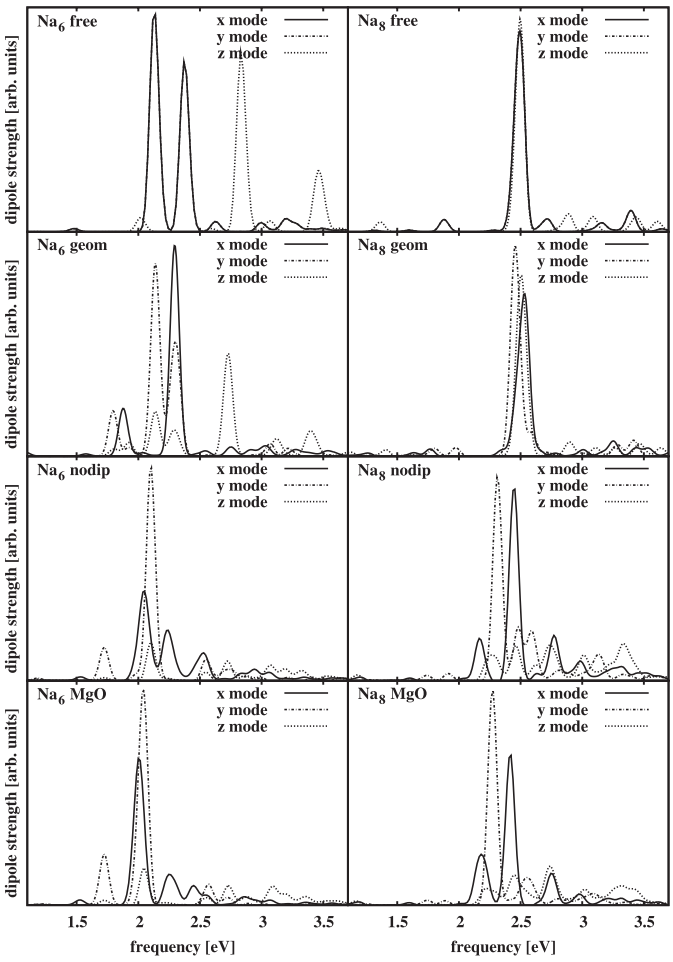

Fig. 3. Optical absorption spectra of Na_6 and Na_8. Various stages of surface contacts are shown (from top to bottom): (i) free cluster, (ii) structure of deposited cluster but without surface interaction, (iii) deposited cluster without dynamical dipole polarization of the surface, (iv) deposited cluster with full interactions.

interfaces. The core repulsion of the contact layer squeezes the tails of the electronic wavefunctions away from the surface and lifts the electronic Kohn-Sham potential by that sizeable amount. This will have a strong effect on the electron dynamics in many respects as, e.g., changed density of single particle states and subsequently changed spectral distributions, as will be discussed in the following section. The dependence of IPs on cluster size shows in the free case the well known odd-even staggering [40]. For deposited clusters, the feature is obviously overruled by surface effects. This finding deserves further detailed investigation.

3.2 Optical response

Optical absorption spectra are among the most important observables in cluster physics. The spectra of metal clusters are dominated by the Mie surface plasmon which concentrates the spectra in a very narrow frequency range.

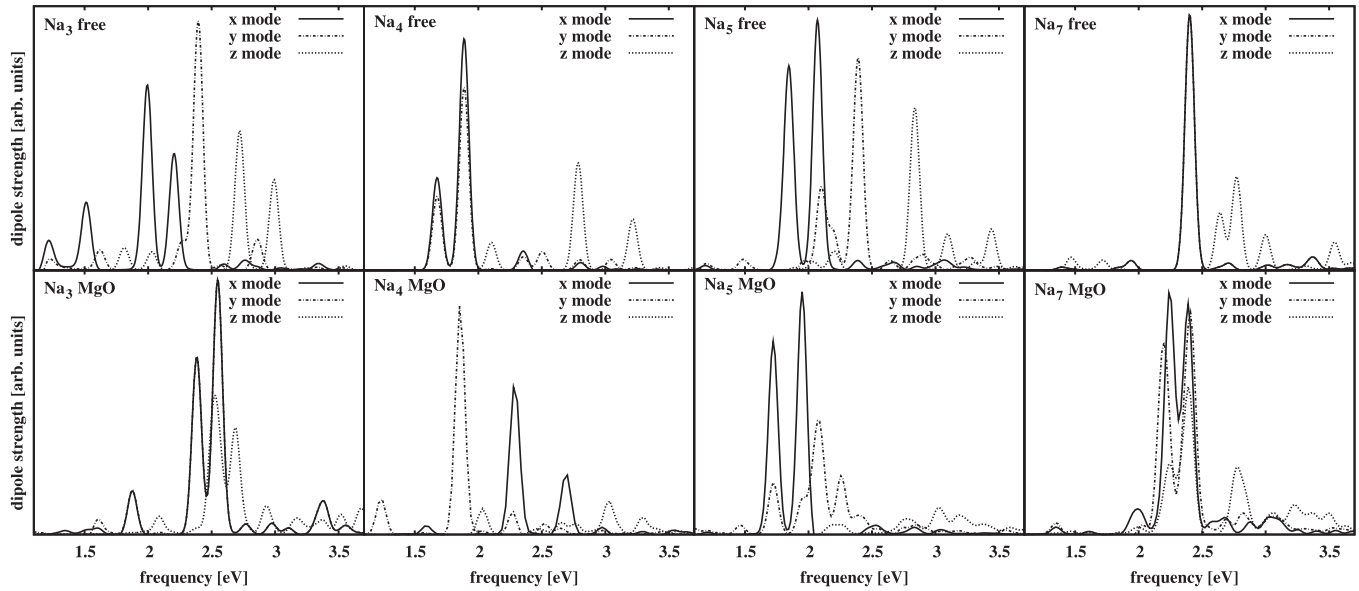

Fig. 4. Optical absorption spectra for Na_N with $N = 3$, 4, 5, and 7. The upper panels show the results for free clusters, the lower panels for deposited ones. The modes in all three directions are shown as indicated.

The average position of the resonance depends on the overall extension (radius), the relative average positions of x, y, and z modes (collective splitting) are related to the global quadrupole deformation, and finer details of the Landau fragmentation emerge from the interference with energetically close one-electron-one-hole states [19]. The present model accounts for the polarization interaction which is most crucial for the response properties of the clusters. Moreover, we find that the cluster electrons do not penetrate into the substrate for ground state and the excitations considered here due to the large (and correctly reproduced) transmission barrier of MgO. Thus one can expect an adequate description of average properties of the cluster's optical response in the resonance region. However, the model does not include an explicit description of the electronic surface states of the substrate (which, for the ideal MgO(001) surface, are anyway rare in the band gap). Therefore, we expect that spectral fragmentation is somewhat underestimated; such details have to be taken with a grain of salt.

Figures 3 and 4 compare spectra of free and deposited clusters. In general, the overall average peak position changes very little. This confirms previous findings that cluster bonding as such still dominates over the interface potential [13,14]; hence, the overall size of the cluster remains robust under deposition. The trends of the collective splitting differ notably among the various clusters. This complies with the results of the structure determination where we have seen that the degree of deformation varies strongly.

Free Na_8 is the most symmetric system of our sample. Its spectrum (upper right panel) is distinguished by near degeneracy of the three modes and by one all dominant Mie resonance. This changes somewhat for deposited Na_8 (lowest right panel in Fig. 3). The main effect is an enhanced spectral fragmentation. Strong changes of the underlying single particle spectrum had already been indicated by the change in the IP (see above). The enhanced spectral density leads to more Landau fragmentation. The effect is particularly dramatic in z-direction. The core repulsion from the surface is fully explored here and it leads to a huge Landau broadening, practically a dissolution, of the Mie resonance. In order to disentangle the influence of the substrate, we have switched it on in steps. The second panel, denoted "geom", shows the case where we use the geometry of the deposited cluster but ignore all surface interactions. This indicates that the shape of deposited Na_8 is neither deformed nor squeezed at all as compared to the free cluster. For the third panel, we have activated the core repulsion from the surface, still omitting the dynamical polarizability (setting $V_{\rm soft} = 0$ in Eq. (4)). This step reduces the IP and thus produces a huge fragmentation of the spectrum. Finally, we activated the full interaction including dynamical polarizability (lowest panel). This even slightly reduces the fragmentation, half-way restoring collectivity. Note that the average peak position hardly changes in all steps although the fragmentation gives often the false impression of such drifts. Altogether we see that core repulsion is the crucial agent in producing the spectral fragmentation.

The same switching of the surface in steps is shown for Na_6 in the left-hand column of Figure 3. The free cluster starts here with a fragmented spectrum with significant collective splitting (cf. z vs. x mode). The nearly axial symmetry leaves x and y modes still perfectly degenerate. The now large change in geometry (Fig. 1) results in more significant changes in the spectrum (second panel) where particularly the x-y degeneracy is broken. Core repulsion leads again to the near dissolution of the z mode and further fragmentation of the x mode, but surprisingly

to a re-concentration of the y mode. This pattern is again only slightly changed by the final step to full surface interaction. The re-concentration of the y mode demonstrates that patterns which depend on spectral details are unpredictable by simple rules. They can go one way or the other because the interplay between single-particle spectra and resonance position is volatile.

The spectra of other clusters are shown without intermediate steps (Fig. 4). The effects remain very similar. The shifts of the average peak positions relate nicely to the (small) changes in structures, the z mode disappears in all cases, and the fragmentation pattern varies strongly and without notable trend as was to be expected. The situation differs from the case of NaCl in which deposited Na clusters experienced a strong oblate deformation leading to a sizeable geometrical splitting of the optical response, even for magic clusters such as Na_8 or Na_{20} [41]. For the MgO substrate, the changes in collective splitting are less important while fragmentation pattern are more affected.

4 Conclusion

We have developed a model for Na clusters on MgO(001) surfaces using a combination of quantum-mechanical description with classical molecular dynamics. The Na cluster is treated by time-dependent density-functional theory in full detail. Classical dynamics is used for the constituents of the more inert substrate, namely Mg^{2+} cations and O^{2-} anions. Care is taken to include the sizeable dynamical polarizability of the anions. This is done in practice by associating two degrees-of-freedom with O^{2-}, a valence electron cloud and the complementing ionic core. The interaction between the substrate ions and the constituents of the Na cluster is described by polarization potentials and a local short-range pseudo-potential to account for effects of core repulsion. For the adjustment of the model parameters, we employ quantum chemical calculations of a Na adsorbate on MgO at a great variety of positions and distances to the surface.

In a first exploration, we have investigated structure and optical response of $Na_N MgO$ for $N = 3 \ldots 8$. The surface interaction is weaker than intra-cluster binding. The overall size of the clusters and their global deformation stay robust under deposition. This is particularly apparent for Na_8 which is well bound due to electronic shell closure. On the other hand, the interaction of the cluster with the surface is strong enough to modify details of structure. Bond angles are adjusted to accommodate the surface corrugation of MgO. The ionization potential is reduced by about 15% for all clusters. This is due to the repulsive part of the interface potential. The optical response shows similarly a coexistence of strong and weak effects. The average peak positions of the Mie plasmon resonances are not shifted. This complies with the robustness of the cluster shape found in the structure calculations. However, the details of the spectrum, namely the spectral fragmentation due to interplay of resonance and nearby single-particle transitions, are strongly modified by deposition.

The great technical simplification brought by the model will allow systematic studies going up to large systems and scanning various dynamical regimes. That will be exploited in the near future.

This work was supported by the Deutsche Forschungsgemeinschaft (RE 322/10-1, RO 293/27-2), Fonds der Chemischen Industrie (Germany), a Bessel-Humboldt prize, and a Gay-Lussac prize.

References

1. *Nanocatalysis*, edited by U. Heiz, U. Landman (Springer, Berlin, 2006)
2. *Chemisorption and Reactivity of Supported Clusters and Thin Films*, edited by R.M. Lambert, G. Pacchioni, NATO ASI Series E (Kluwer, Dordrecht, 1997), Vol. 331
3. K. Watanabe, D. Menzel, N. Nilius, H.J. Freund, Chem. Rev. **106**, 4301 (2006)
4. H.J. Freund, M. Bäumer, H. Kuhlenbeck, Adv. Catal. **45**, 333 (2000)
5. N. Rösch, V.A. Nasluzov, K.M. Neyman, G. Pacchioni, G.N. Vayssilov, in *Computational Material Science*, edited by J. Leszczynski (Elsevier, Amsterdam, 2004), Theoretical and Computational Chemistry Series, Vol. 15, p. 367
6. C. Binns, Surf. Sci. Rep. **44**, 1 (2001)
7. Appl. Phys. A **82** (2006), topical issue on "Clusters in Contact with Surfaces", edited by K.M. Meiwes-Broer
8. *Metal Clusters*, edited by W. Ekardt (Wiley, New York, 1999)
9. A. Sanchez, S. Abbet, U. Heiz, W.D. Schneider, H. Häkkinen, R.N. Barnett, U. Landman, J. Phys. Chem. **103**, 9573 (1999)
10. T. Götz, F. Träger, M. Buck, C. Dressler, F. Eisert, Appl. Phys. A **60**, 607 (1995)
11. H. Häkkinen, M. Manninen, J. Chem. Phys. **105**, 10565 (1996)
12. C. Kohl, P.G. Reinhard, Z. Phys. D **39**, 225 (1997)
13. F. Fehrer, P.G. Reinhard, E. Suraud, E. Giglio, B. Gervais, A. Ipatov, Appl. Phys. A **82**, 151 (2005)
14. F. Fehrer, P.G. Reinhard, E. Suraud, Appl. Phys. A **82**, 145 (2005)
15. N. Gresh, O. Parisel, C. Giessner-Prettre, Theochem **458**, 27 (1999)
16. P.J. Mitchell, D. Fincham, J. Phys.: Condens. Matter **5**, 1021 (1993)
17. V.A. Nasluzov, K. Neyman, U. Birkenheuer, N. Rösch, J. Chem. Phys. **115**, 17 (2001)
18. B. Gervais, E. Giglio, E. Jaquet, A. Ipatov, P.G. Reinhard, E. Suraud, J. Chem. Phys. **121**, 8466 (2004)
19. P.G. Reinhard, E. Suraud, *Introduction to Cluster Dynamics* (Wiley, New York, 2003)
20. F. Calvayrac, P.G. Reinhard, E. Suraud, C.A. Ullrich, Phys. Rep. **337**, 493 (2000)
21. F. Fehrer, M. Mundt, P.G. Reinhard, E. Suraud, Ann. Phys. (Leipzig) **14**, 411 (2005)
22. C. Legrand, E. Suraud, P.G. Reinhard, J. Phys. B **35**, 1115 (2002)
23. S. Kümmel, M. Brack, P.G. Reinhard, Eur. Phys. J. D **9**, 149 (1999)

24. D.E. Parry, Surf. Sci. **49**, 433 (1975)
25. D.E. Parry, Surf. Sci. **54**, 195 (1976)
26. M. Winkler, Diploma thesis, Technische Universität München (2006)
27. B.I. Dunlap, N. Rösch, Adv. Quantum Chem. **21**, 317 (1990)
28. T. Belling, T. Grauschopf, S. Krüger, M. Mayer, F. Nörtemann, M. Staufer, C. Zenger, N. Rösch, in *High Performance Scientific and Engineering Computing*, edited by H.J. Bungartz, F. Durst, C. Zenger (Springer, Heidelberg, 1999), Lecture Notes in Computational Science and Engineering, Vol. 8, p. 441
29. T. Belling, T. Grauschopf, S. Krüger, F. Nörtemann, M. Staufer, M. Mayer, V.A. Nasluzov, U. Birkenheuer, A. Hu, A.V. Matveev et al., ParaGauss, Version 3.1, Technische Universität München (2004)
30. P. Widmark, B. Persson, B. Roos, Theor. Chim. Acta **79**, 419 (1991)
31. A. Becke, Phys. Rev. A **38**, 3098 (1988)
32. J. Perdew, Phys. Rev. B **33**, 8822 (1986)
33. L.H. Tjeng, A.R. Vos, G.A. Sawatzky, Surf. Sci. **235**, 269 (1990)
34. V. Blum, G. Lauritsch, J.A. Maruhn, P.G. Reinhard, J. Comp. Phys **100**, 364 (1992)
35. M.D. Feit, J.A. Fleck, A. Steiger, J. Comp. Phys. **47**, 412 (1982)
36. F. Calvayrac, P.G. Reinhard, E. Suraud, Ann. Phys. (N.Y.) **255**, 125 (1997)
37. C. Inntam, L.V. Moskaleva, K.M. Neyman, V.A. Nasluzov, N. Rösch, Appl. Phys. A **82**, 181 (2006)
38. A.M. Ferrari, C. Xiao, K.M. Neyman, G. Pacchioni, N. Rösch, Phys. Chem. Chem. Phys. **1**, 4655 (1999)
39. S. Cai, K.M. Neyman, A. Hu, N. Rösch, J. Phys. Chem. B **104**, 11506 (2000)
40. M. Manninen, J. Mansikka-aho, H. Nishioka, Y. Takahashi, Z. Phys. D **31**, 259 (1994)
41. C. Kohl, F. Calvayrac, P.G. Reinhard, E. Suraud, Surf. Sci. **405**, 74 (1998)